

Dissolution of steel slags in aqueous media

Shashikant Yadav¹ · Anurag Mehra¹

Received: 18 July 2016 / Accepted: 13 April 2017 / Published online: 25 May 2017
© Springer-Verlag Berlin Heidelberg 2017

Abstract Steel slag is a major industrial waste in steel industries, and its dissolution behavior in water needs to be characterized in the larger context of its potential use as an agent for sequestering CO₂. For this purpose, a small closed system batch reactor was used to conduct the dissolution of steel slags in an aqueous medium under various dissolution conditions. In this study, two different types of steel slags were procured from steel plants in India, having diverse structural features, mineralogical compositions, and particle sizes. The experiment was performed at different temperatures for 240 h of dissolution at atmospheric pressure. The dissolution rates of major and minor slag elements were quantified through liquid-phase elemental analysis using an inductively coupled plasma atomic emission spectroscopy at different time intervals. Advanced analytical techniques such as field emission gun-scanning electron microscope, energy-dispersive X-ray, BET, and XRD were also used to analyze mineralogical and structural changes in the slag particles. High dissolution of slags was observed irrespective of the particle size distribution, which suggests high carbonation potential. Concentrations of toxic heavy metals in the leachate were far below maximum acceptable limits. Thus, the present study investigates the dissolution behavior of different mineral ions

of steel slag in aqueous media in light of its potential application in CO₂ sequestration.

Keywords CO₂ sequestration · Slag carbonation · Slag dissolution · Silica film · Slag stabilization · Incongruent dissolution

Introduction

There is a growing interest in mineral CO₂ sequestration, also called mineral carbonation, especially in regions where there is a scarcity of natural resources or feasibility issues for geological sequestration (Koljonen et al. 2004; Sipilä et al. 2008). The majority of mineral CO₂ sequestration research is focused on the carbonation of natural alkaline earth minerals. However, significant success has also been achieved in carbonation with other solid alkaline waste materials (Lekakh et al. 2008; Gunning et al. 2010; Sanna et al. 2014). There are different types of solid alkaline waste materials available with a high composition of calcium (Ca) and magnesium (Mg). Municipal solid waste (MSW), industrial by-products such as steel slags, coal fly ash and cement-based waste materials possess high concentrations of Ca and Mg and are therefore potential sequestration raw materials (Huijgen and Comans 2005; Revathy et al. 2015; Ghacham et al. 2016).

The steel industry produces a huge quantity of slags which accounts for 10 to 15% of the weight of the manufactured steel (Proctor et al. 2000). Global steel production is at 1.65×10^3 Mt/year, with Asia and Europe being the largest producers accounting for 1.12×10^3 and 2.05×10^2 Mt, respectively (Costa et al. 2016). The total iron and steel slag produced is roughly about 480 to 620 Mt/year which can be used for CO₂ sequestration (van Oss 2015). The storage potential of the steel slag is estimated to be 96–145 Mt CO₂/year

Responsible editor: Philippe Garrigues

✉ Anurag Mehra
mehra@iitb.ac.in

Shashikant Yadav
shashikant529@gmail.com

¹ Department of Chemical Engineering, Indian Institute of Technology Bombay, Powai, Mumbai 400076, India

(Teir et al. 2007). Also, the carbonate end product has other industrial benefits as well (Sipilä et al. 2008).

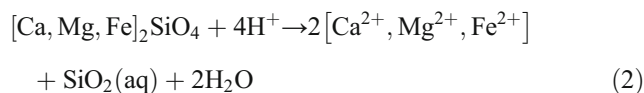
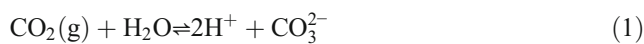
Steel slag production is reasonably constant throughout the year and across the country. Steel slag is also economical and of reliable quality. Besides, steel slag demonstrates high reactivity due to chemical instability caused by the industrial process of high-temperature production followed by rapid cooling (Huijgen and Comans 2005; Huijgen et al. 2006; Baciocchi et al. 2009). Further, due to its relatively porous structure, steel slags possess high surface area than natural alkaline earth minerals. All these advantages make steel slag a suitable feedstock for CO₂ sequestration.

Over the past few years, extensive studies have been conducted on the CO₂ sequestration methods to assess or increase the sequestration potential and/or accelerate the reaction rate. These studies include changing reaction parameters such as temperature and pressure conditions (Huijgen et al. 2005; Bonenfant et al. 2008; Bobicki et al. 2012). It also includes studies that have explored the effect of additives usage or changes to the reaction medium composition (Bao et al. 2010; Gunning et al. 2010; Chang et al. 2013). Furthermore, there have been studies conducted on the use of the resultant product of carbonation (Eloneva et al. 2012; Santos et al. 2012; Sorlini et al. 2012), landfilling (Diener et al. 2010), and their environmental impact (Huntzinger and Eatmon 2009; Pan et al. 2013; Xiao et al. 2014).

Slag carbonation has been extensively investigated for both direct and indirect aqueous carbonation routes. Direct aqueous carbonation can be conducted either as slurry phase carbonation (Bonenfant et al. 2008; Lekakh et al. 2008) or as wet phase carbonation (van Zomeren et al. 2011). The major challenge in direct aqueous mineral carbonation is the slow reaction kinetics. However, the use of several additive chemicals increases the carbonation reaction rate (O'Connor et al. 2000; Huijgen and Comans 2003; O'Connor et al. 2005). Though indirect aqueous carbonation has sufficient reaction rate, additive chemicals are used to extract the reactive compounds from the steel slag at a low pH level in the first step followed by the carbonation reaction at a high pH level in a separate second step (Park and Fan 2004; Teir et al. 2007).

Additive chemicals enhance the carbonation process, but they tend to increase the dissolution of toxic mineral ions during the reaction, which may pose an environmental hazard in disposal and re-use (Kasuura et al. 1996; Hong and Tokunaga 2000; Quina et al. 2008). Similarly, complete recovery and recycling of the additive chemicals are necessary to make this process economically feasible. There are no data to support the argument that the use of additives can be energy-efficient and economical. This suggests that carbonation process simply using an aqueous suspension of slag without any additives may have enormous sequestration potential.

The interaction between the steel slag and the CO₂ is described by the following reactions:



The carbonation process involves the reaction of the three constituents which are water, steel slag, and CO₂. The complete carbonation reaction takes place simultaneously in three steps as explained in Eqs. 1–4. They are (i) dissolution of CO₂ and steel slag within the water (Eqs. 1 and 2), (ii) the reaction between dissolved steel slag and CO₂ present in the aqueous solution (Eq. 3), and (iii) the precipitation of products obtained from the carbonation reaction (Eq. 4). Among these, the dissolution of steel slag (Eq. 2) is the rate-determining step of the CO₂ sequestration process (Daval et al. 2009; Bonfils et al. 2012).

It, therefore, becomes relevant to study the dissolution of steel slag under different conditions. The base or reference study is the dissolution of the slag in water just by itself without anything else being present. Subsequent studies can then be carried out in the presence of CO₂. Considerable literature is available on the chemically enhanced dissolution of steel slag, where additives such as acetic acid, nitric acid, and hydrochloric acid are used to increase dissolution rate (Bao et al. 2010; Olajire 2013; Sanna et al. 2014). However, only limited literature is available on pure aqueous dissolution of slag without the use of any additives (De Windt et al. 2011; Li et al. 2012). The former study investigated the dissolution of steel slag, using different concentrations of slag, at ambient conditions; the effects of particle size and temperature were not studied. The latter study investigated the leaching characteristics of Ca, Si, and Al and their effects on cementitious properties of steel slag using a fixed bed reactor and did not explore the effects of temperature, particle size, and concentration of steel slag. Subsequently, Pan et al. also studied dissolution and carbonation of basic oxygen furnace slag (BOFS) but in separate reactors. In their experiment, a part of carbonated slag recycled to the dissolution reactor (Pan et al. 2013). However, in this study, due to the mixing of fresh and carbonated slag in the dissolution process, individual kinetic of leaching of slag cannot be accurately estimated. In the present study, the dissolution rate of the slag is measured in an aqueous phase at different temperatures, particle sizes, and solid to liquid (S/L) ratios. The objectives include understanding dissolution mechanisms and the effects of the dissolution process on the mineralogical changes in the dissolved slag. This study

Table 1 Mineral composition of fresh steel slag based on XRF analyses (wt%)

Sample	Al ₂ O ₃	CaO	Cr ₂ O ₃	FeO	P ₂ O ₅	SiO ₂	TiO ₂	SO ₄	V ₂ O ₅	MgO	MnO
Slag-1	6.113	34.287	0.091	31.579	1.183	16.055	0.707	0.168	0.124	6.334	0.672
Slag-2	5.661	45.761	0.098	20.928	1.918	15.08	0.777	0.643	0.035	6.026	0.702

essentially explores how “easily” slag releases its components into an aqueous phase and which species dissolve relatively faster than others.

Materials and methods

Sample preparation

Experiments were conducted in batch reactors to quantify the dissolution rate of steel slags within an aqueous medium. The materials used in the experiment were basic oxygen furnace (BOF) slags sourced from two different Indian steel plants. Initially, samples of steel slags were hammer crushed and with the help of a ball mill were ground into fine powder. Depending on the size, the samples were separated using sieve agitator. Accordingly, samples of three ranges of size were selected for the study: 25–37, 37–53, and 53–75 μm. For the experiment, samples were prepared by an acetone wash and 10-min sonication, which removed fine particles from the sample. In order to cleanse and clarify the material, acetone was removed from the sample, and the acetone wash was repeated. The entire process was repeated five times to ensure the removal of all fine particles. Further, the samples were cleansed with water and then dehydrated in an oven for 24 h at a temperature of 105 °C to ensure complete dehydration. The washed samples were analyzed with field emission gun-scanning electron microscope (FEG-SEM) in tandem with EDX technology, which revealed that most of the fine matters were removed and only small traces, on the surface of large particles, remained. The specific surface area (SSA) and porosity were calculated through BET analysis.

Mineralogical characterization

An XRF device (PANalytical PW-2404) was utilized along with an X-ray diffractometer (XRD) (SMART APEXII) to analyze the mineral and chemical composition of the solid slag samples as shown in Tables 1 and 2. The XRD patterns were determined in the 2θ from 10° to 90°. An FEG-SEM instrument (JEOL JSM-7600F) was used in the analysis for the morphological and chemical composition of the precipitates. The JEOL JSM-7600F is a high-resolution, 3-D imaging device with energy-dispersive X-ray (EDX) capabilities. During analysis, samples were coated with gold to eliminate

the charging effect. The PSD analyzer used was Malvern Mastersizer 2000, which utilizes laser diffraction technique. It was used to measure particle size distribution as well as the average size of the slag particles. Inductively coupled plasma atomic emission spectroscopy (ICP-AES) was employed to evaluate the elemental composition of the liquid samples.

Each type of slag is a heterogeneous material defined by its crystalline phase blend. The XRD analysis identifies solid crystalline phases which are given in Table 2. Additional phases were found but could not be identified due to the low intensity of their diffraction lines and the complex nature of the diffractogram.

Experimental method

The experiments were conducted in an air-tight batch reactor with joints sealed by silicon grease and Teflon tape for added protection against leakage. The reactor was immersed in a heating bath which used silicon oil as a heating medium as shown in Fig. 1. Silicon oil was selected due to its high thermal conductivity and boiling point. The reactor allows a high level of temperature control and provides continuous pH measurement via a pH meter. The maximum heat range of the controller was 250 °C. The reactor contained 300 ml of Millipore water. When the desired temperature was attained, the slag was placed inside the reactor. A magnetic stirrer with a speed range of 0 to 2200 rpm was used to control mixing of the material and hold the solids in a suspended state. The time standard used throughout the experiments was 240 h of dissolution at various S/L ratios which were obtained by mixing 0.5, 2, and 5 g of slag in 300 ml water. The experiments were conducted at atmospheric pressure, and the reaction temperatures were 25, 50, and 90 °C.

Slurry samples were collected from the reactor at specific intervals in order to quantify the total amount of minerals dissolved in the solution. The suspended solid particles were

Table 2 Mineral composition of fresh steel slag based on XRD analyses

Materials	Minerals
Slag-1	CaO, MgO, FeO, Fe ₂ O ₃ , Ca(OH) ₂ , Mg(OH) ₂ , SiO ₂ , Al ₂ O ₃ , Fe ₃ O ₄ , Ca ₂ SiO ₄ , Ca ₂ MgSi ₂ O ₇ , Mg ₂ SiO ₄ , Ca ₂ FeAlO ₅
Slag-2	CaO, MgO, Fe ₂ O ₃ , Ca(OH) ₂ , Mg(OH) ₂ , Ca ₂ SiO ₄ , CaCO ₃ , SiO ₂ , Al ₂ O ₃ , Ca ₂ Fe ₂ O ₅ , CaAl ₂ Si ₂ O ₈ , Ca ₂ Fe ₂ O ₅ , MgCr ₂ O ₄

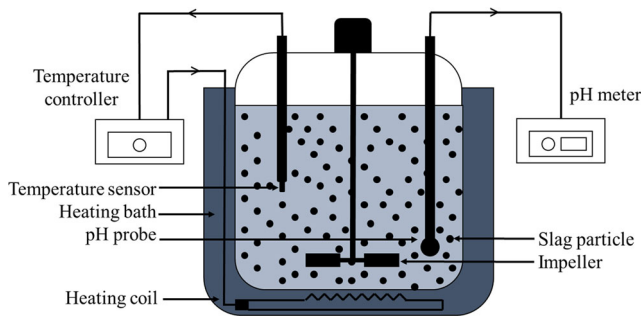


Fig. 1 Schematic diagram of the reactor

extracted from the sample with a filter having an opening size of 0.2 μm . The filtrates which contained dissolved elements were diluted with nitric acid as a preventive measure against precipitation. Further, vaporization of the filtrate was also arrested by containing it in air-sealed bottles. The samples from filtrate were analyzed for elemental analysis using ICP-AES to evaluate the concentration of numerous mineral ions, such as Fe, Ca, Si, Mg, Mn, Zn, Al, V, Cd, Sb, As, Se, Hg, Pb, Cu, Mo,

Co, S, Br, P, Sn, Cr, Sr, Ba, and Ni, which is indicative of the dissolution characteristics of the slag. The separated solid samples were oven dried for 24 h, stored in air-tight bottles and were examined using morphological and compositional analysis instruments, namely, XRD, FEG-SEM, and BET.

Results and discussion

Dissolution behavior of slag

In the present study, the effects of particle size, slag composition and solution temperature on the dissolution rate were investigated. Among major elements, such as Ca, Fe, Si, Al, Mg, Mn, Ti, and P, Ca leached the most and Al the least. Figure 2 depicts the variation in concentrations of the Ca ions with time for different slag compositions, solution temperatures, and particle size distribution. Steel slag consisted of two types of minerals: (i) easily dissolvable (e.g., CaO, MgO, and

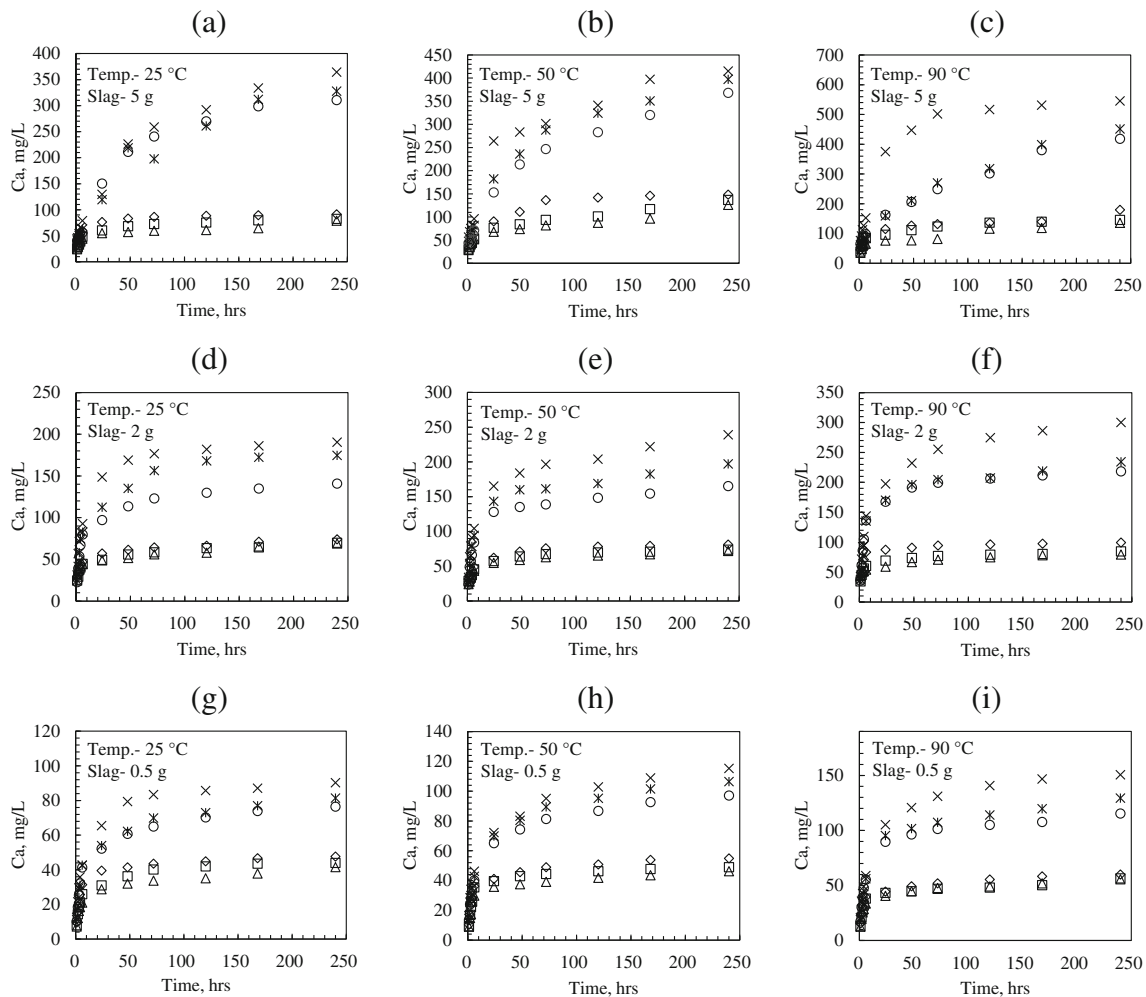


Fig. 2 Change in concentration of Ca in the leachate with time. The symbols representation are as follows: **i** slag-1, 25–37 μm (empty triangle); **ii** slag-1, 37–53 μm (empty square); **iii** slag-1, 53–75 μm

(empty triangle); **iv** slag-2, 25–37 μm (multiplication sign); **v** slag-2, 37–57 μm (empty square), slag-2, 53–75 μm (empty circle)

Ca(OH)₂) and (ii) difficult to dissolve (e.g., Ca₂Fe₂O₅, Ca₂SiO₄, Ca₃Mg(SiO₄)₂, and Ca₂MgSi₂O₇) (Lackner et al. 1997; Huijgen and Comans 2005; Bao et al. 2010). The rate of dissolution varied hugely between the slags that were procured from two different sources. Slag-2 was found to have a much higher Ca dissolution rate across all slag compositions, solution temperatures and particle size distribution. Ca dissolution from slag-2 increased rapidly for over 48 h under all conditions due to the presence of highly soluble minerals (e.g.,

CaO and Ca(OH)₂) within the steel slag. The rate of Ca dissolution in slag-2 then decreased gradually and became stagnant after about 168 h under all conditions. However, in slag-1, the Ca dissolution showed a flatter trajectory over time under all conditions compared to slag-2 as is evident from Fig. 2. It can also be seen that the Ca concentration under similar conditions is considerably lower for slag-1 compared to slag-2 due to the low initial Ca composition in slag-1. From Figs. 2 and 3a, b, it can be observed that dissolution rate of Ca

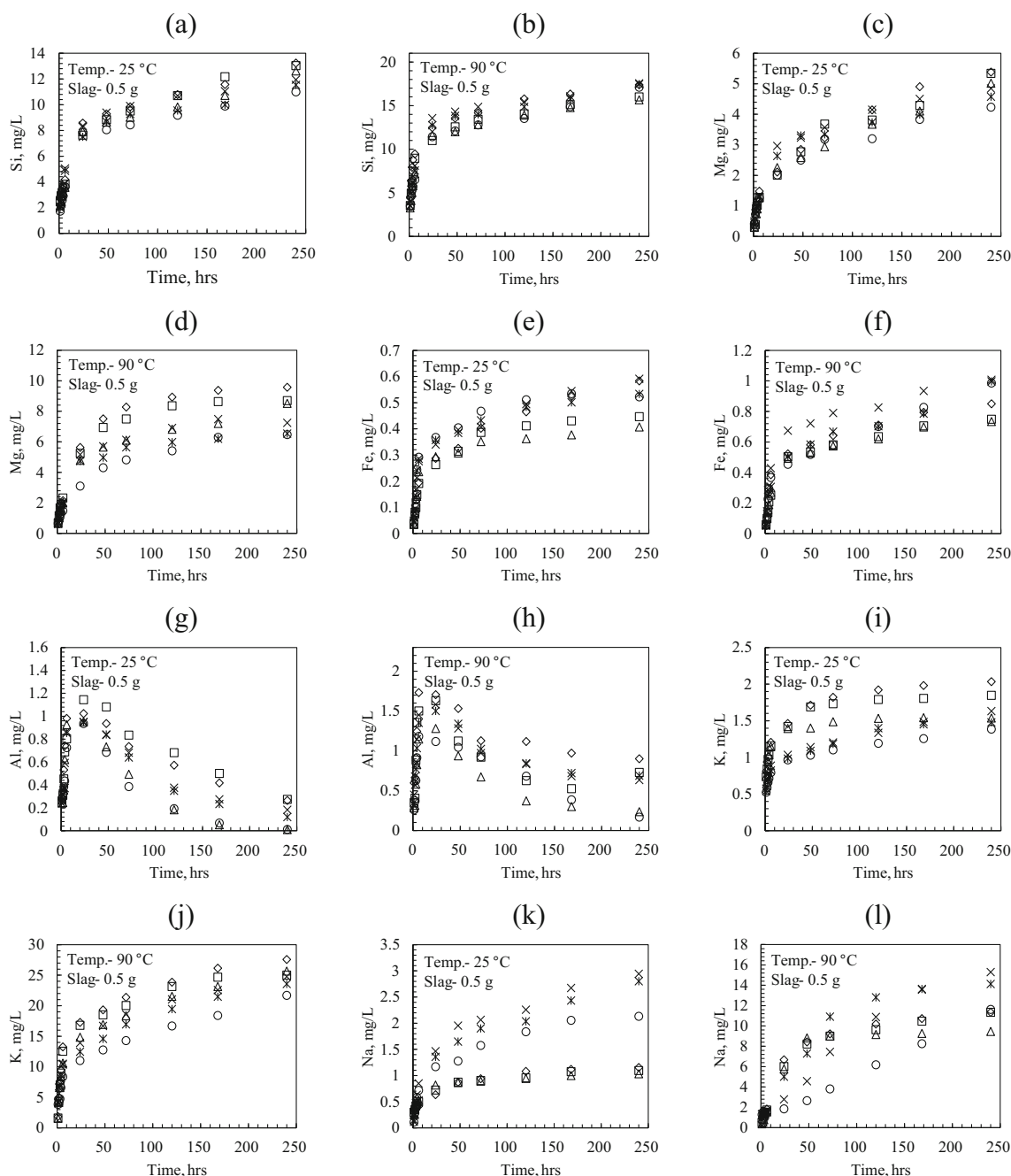


Fig. 3 Change in concentration of Si, Mg, Fe, Al, K, and Na in the leachate with time. The symbols representation are as follows: **i** slag-1, 25–37 μm (empty diamond); **ii** slag-1, 37–53 μm (empty square); **iii** slag-

1, 53–75 μm (empty triangle); **iv** slag-2, 25–37 μm (multiplication sign); **v** slag-2, 37–57 μm (empty square)

is higher compared to Si, which can be attributed to increased resistance in the latter as the dissolution of slag forms a new silica-rich layer on the surface of the slag particles because of incongruent dissolution. A peculiar leaching behavior was observed for Al as shown in Fig. 3g, h in which concentration increases during the first 6 h at 90 °C and 24 h at 25 °C and then starts gradually declining and reaches a minimum level by the end of 240 h. This trend indicates the precipitation of secondary compounds such as $H_4Al_2O_5$.

Morphological and compositional changes

Morphological and compositional changes in the slag after 240 h of dissolution were investigated by advanced analytical techniques such as XRD and SEM/EDS. Figures 4 and 5 depict the scanning micrographs of the steel slag after 240 h of dissolution. During the dissolution, the soluble minerals in the slag were dissolved whereas the insoluble minerals formed a residual layer on the surface of the particle. In Fig. 4, evidence of incongruent dissolution can be seen due to the highly porous surface of undissolved minerals (primarily SiO_2). Figure 4a depicts the outer surface of the particles at 50 μm magnification and Fig. 4b a closer view of the outer surface of a single particle at 20 μm magnification, respectively. Figure 4c shows that some particles start to crack during dissolution process and post 240 h of dissolution, slag particles become highly porous as shown in Fig. 4d. This incongruent dissolution was also confirmed by elemental analysis of the slag after dissolution reaction using SEM–EDS and, similarly, compositional analysis by XRD, which confirmed the formation of silica (SiO_2).

In the unreacted fresh slag particle, the fraction of Ca was high. Once the dissolution process starts, Ca is significantly leached from the slag particles. Due to leaching of Ca, the Ca–silicate core was reduced and enclosed by a Ca-depleted undissolved residue layer. Figure 5 depicts this silica-rich surface that is formed due to the incongruent dissolution. It is evident that the residue layer which mainly comprised of SiO_2 further retards the diffusion of Ca from within the particle, which causes a reduction in the rate of dissolution. Simultaneously, the thickness of the undissolved residue layers increased with time, which caused an increase in resistance to mass transfer causing an even further reduction in the dissolution rate of slag with time.

Fragile precipitate layers were also formed on the surface of slag particle as a result of the precipitation of secondary compounds which were formed during the dissolution process as shown in Fig. 4c. These precipitate layers provide added strength to the solid particle, which makes them even more resistant to breakage and combined with Ca-depleted residue layers cause further resistance to the release of mineral ions from slag particles to bulk liquid (Butt et al. 1996). However, SEM images reveal that the precipitate layer was still fragile. It grows to a certain thickness and then fractures appear on the surface of the layer. New surfaces for solid–liquid interaction

are therefore spawned when attrition force fragments these fragile precipitate layers. Similar behavior was observed by Squires and Wolf (2006) where fracture and exfoliation of carbonate layer were observed due to particle shattering.

It can therefore be concluded from the aforementioned behavior that the dissolution of steel slag resembles the shrinking core model. In this model, steel slag dissolves into the solution leaving behind undissolved residue layer. As reaction proceeds, the interface between unreacted slag and residue starts moving towards the center of the particle. Therefore, the thickness of the residue layer increases, and unreacted slag core shrinks with time. A thin layer of precipitates also forms on the surface of slag particle, as shown in Fig. 4. This model observed two diffusion resistances, one due to the residue layer, and another due to the precipitate layer. Therefore, the evidence shows that the rate of change in the dissolution of mineral ions is controlled by the thicknesses and resistivities of these layers during reaction time.

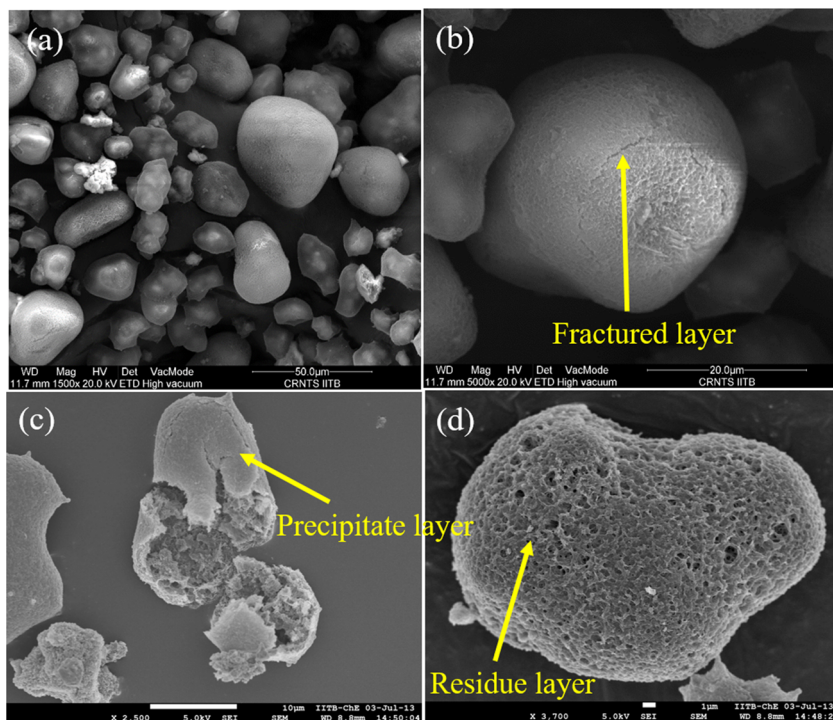
Influence of reaction parameters

The following section reports the experimental results of steel slag dissolution involving changes to the parameters: temperature, S/L ratio, and particle size. This study also investigates the effect of these parameters on the leaching behavior of steel slag and identifies the most influencing parameter for steel dissolution.

Influence of temperature

Temperature was found to be the critical experimental condition for slag dissolution which has more influence than other parameters. The experiments were performed at three temperatures, 25, 50, and 90 °C, to study the effect of temperature on the dissolution of the slag. Figures 2 and 3a, b illustrate the variation in concentrations of Ca and Si with time at different temperatures. Ca and Si show high dissolution rates at higher temperatures regardless of the S/L ratio. High concentration is also due to the fact that some compounds such as Ca_2SiO_4 and Ca_2FeAlO_5 start dissolving only at higher temperatures. Similar behavior was also described by Pan et al. in their experiments where the dissolution of $CaSiO_3$, Ca_2SiO_4 , and $Ca_2Fe_{1.014}Al_{0.986}O_5$ did not take place at room temperature but at much higher temperatures (Pan et al. 2013). Figure 3c–h illustrates the variation in concentrations of Mg, Fe, and Al (other potential elements to form carbonates) with time. Despite having a significant concentration of Fe and Al in the slag composition, the concentration of Fe and Al was found to be negligible in the solution at all temperatures. However, in the case of Mg, the post-dissolution concentration was substantially more than that of Fe and Al. It was observed that the final concentration of Mg increased from 5.4 to 9.6 mg/L with an increase in temperature from 25 to

Fig. 4 SEM images of slag-2 after 240 h of dissolution. **a** outer surface of the particle. **b** cracks observed in the magnified image of the particle. **c** fragmented particle. **d** porous particle after dissolution reaction



90 °C, which indicates significant influence of temperature on Mg dissolution. Figure 3i–l depicts the concentrations of minor constituents such as Na and K in the solvent with time. As can be noted, temperature significantly impacts Na dissolution as the final concentration of Na was found to be 11.3 mg/L at 90 °C compared to 1.2 mg/L at 25 °C. Similarly, the dissolution of K was also starkly influenced by the increase in temperature.

Influence of S/L ratio

Figure 6a, b demonstrates the typical variation in the final concentration (C_{final}) of various elements (Ca, Mg, and Si) of the solute present in the solvent with the S/L ratio. Figure 6a shows the relationship for the experiment conducted with various particle sizes (25–37, 37–53, and 53–75 μm) and Fig. 6b illustrates the relationship for the experiment conducted at different temperatures (25, 50, and 90 °C). It can be observed that final concentration of the elements increased with the increase in S/L ratio. Further, the trend in variation in final concentration of the solute with S/L ratio was found to be identical for all the mineral ions. However, C_{final} of the Ca was observed to be highest at the S/L ratio equal to 0.016, which can be attributed to its higher solubility characteristics in the aqueous medium. Further, a higher final concentration of the elements at the 90 °C in comparison to 25 °C suggests the use of higher temperature during the dissolution, even though increase is not proportional.

Influence of particle size

Figure 6a illustrates the variation in the final concentration (C_{final}) of mineral ions in the solution with S/L ratio for the slags having three different ranges of particle size (25–37, 37–53, and 53–75 μm). Figure 6 shows that increase in the particle size causes a decrease in the final concentration of the mineral ions, which can be attributed to hindrance in the dissolution of the bigger particles due to their lesser total surface area. Figure 6 also reveals that the effect of particle size is more for Ca concentration than for other mineral ions, and also, the effect is more pronounced at higher S/L ratios. It can be noted that for each particle size range, dissolution of the slag particles increased with the increase in the S/L ratio, but the increase is not proportional.

Significance of dissolution of ions in CO₂ sequestration

In the present study, the dissolution behavior of different mineral ions of steel slag in aqueous media was investigated to predict their potential in the CO₂ sequestration. Carbonates formed by each mineral ion have unique chemical properties. Mineral ions, like Ca, Mg, Fe, and Al, present in significant amount in both the slags, have the property to form chemically stable carbonates (Huijgen and Comans 2003; Teir 2008). Similarly, Na, K, and Li present in small quantities also form bicarbonates when they react with CO₂ (IPCC 2005). However, carbonates of these mineral ions are reported to be chemically unstable and prone to decomposition into primary

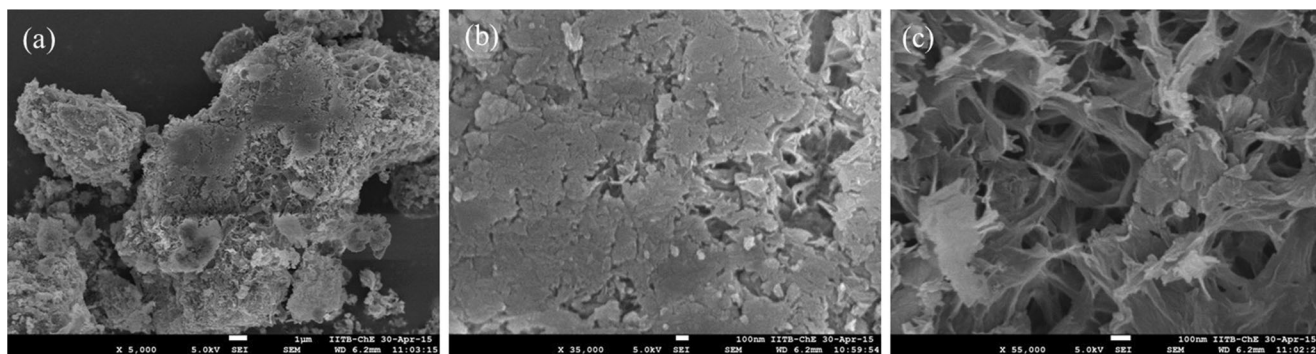


Fig. 5 SEM images of Slag—1 after 240 hours of dissolution

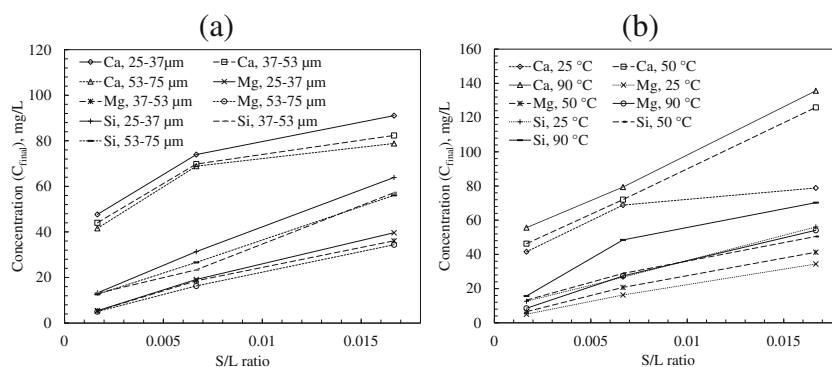
ions in the aqueous environment (Teir 2008; Pan et al. 2012). Despite the tendency of Fe and Al to form stable carbonates and their initial large slag composition availability, their concentration in solution was found to be negligible. This underlines their low dissolution capacity and highlights the reduced potential to form carbonates and subsequently contribution in CO₂ sequestration. Likewise, Ti and Mn, which also have the potential to form stable carbonates and present in a noticeable amount in the initial slags, their concentration in the leachate was negligible. Though K, Na, and Li display dramatically higher dissolution rates at higher temperatures, their propensity to form unstable carbonates as mentioned earlier makes them prone to CO₂ leakage quite easily (IPCC 2005). Their instability, despite their dissolution performance, makes them unsuitable for sequestration. Ca and Mg showed significant dissolution even at low temperatures, suggesting their potential use for CO₂ sequestration. These results suggest that Ca and Mg are the only candidates that have the capability to form stable carbonates and have sufficient dissolution rates to be considered for CO₂ sequestration. Though precipitation of calcium carbonate is possible under atmospheric pressure, magnesium carbonate precipitates only under high pressure (Huijgen et al. 2005). Hence, based on the above results, it can be stated that CO₂ sequestration can be accelerated by using slag containing a high fraction of Ca and Mg provided the necessary condition of high pressure is used. However, maintaining a high-pressure condition in field applications may not be economically viable. Hence, conclusively, usage

of steel slag having high Ca fraction is the only viable option to enhance the potential to form stable carbonates and sufficient dissolution of mineral ions even under normal reaction conditions for effective CO₂ sequestration.

Presence of heavy metals

Dissolution of steel slag in aqueous media and the subsequent CO₂ sequestration involves the dissolution of various minerals including heavy metals in the process. Since dissolution of toxic heavy metals is an environmental concern due to growing environmental awareness, steel slag dissolution process is investigated from that perspective as well. The concentration of these heavy metals, which are minor elements, was quantified at different time intervals and their values were compared with the maximum permissible limits, as defined by the Central Pollution Control Board (CPCB) (CPCB 2006). At 25 °C, the concentration of these mineral ions remains lower than the maximum permissible value. However, the concentration increased at higher temperatures. But, the recorded values for all the elements still remained well within the CPCB standards. This shows that CO₂ sequestration methods without the use of additives have a lower leaching rate of toxic metals compared to those with the use of additives, even though some studies suggest that the carbonated steel slag has a higher leaching rate for some of the heavy metals (Morone et al. 2016).

Fig. 6 Effect of S/L ratio on the total dissolved concentration of Ca, Mg, and Si for slag-1. **a** Variation in total concentration with different particle size ranges at 25 °C. **b** Variation in total concentration with temperature for particle size ranges 53–75 μm



Stabilization of steel slag

The presence of highly reactive components such as mineral oxides and leachable toxic heavy metals in the steel slag makes it unsuitable for direct discharge into landfills or usage in construction materials (Johnson et al. 1995; Yan et al. 1997). The pH of the solution increased sharply from 9 to 9.5 for both slags within 30 min, as compared to the initial pH value of 7, observed before addition of slag. This sudden increase in pH of the solution can be attributed to high dissolution of the mineral ions through steel slag in the initial stages of the reaction. However, the dissolution rate was found to decline and almost cease after the duration of 120 h. The sudden increase in pH also highlights its hazardousness for direct disposal into landfills which can severely affect living organisms and disrupt their ecosystem (Bertos et al. 2004). This suggests that minimum 120 h of carbonation is required under standard operating conditions to stabilize the steel slag before its usage in landfills. Additionally, when the untreated steel slag is disposed as a waste material in open space, it undergoes the natural weathering process (Yan et al. 1997). During this process, reactive components present within the slag, such as mineral oxides, are converted into minerals carbonates (Yuen et al. 2016). The change in composition of the steel slag leads to change in the volume of slag with time which in turn makes it unsuitable for use in construction industry. However, carbonation process can be employed for neutralizing the reactive oxides and converting them into thermodynamically stable carbonates (Johnson et al. 1995; Bertos et al. 2004) which improve their physical properties making the carbonated slag suitable both for landfills and for industrial applications (Sahu et al. 2010).

Conclusion

The dissolution of slags was studied using a batch slurry reactor, containing steel slag and water. The concentration of mineral ions in the solution during the dissolution experiments was used to explore the influence of the various parameters such as type of the slags, temperature, particle size, and S/L ratio. Further, advanced analytical techniques such as SEM–EDX, XRD, and ICP were also used to investigate the morphological, structural, and chemical compositions of the slag at various time intervals.

High dissolution was observed irrespective of the particle size distribution. Selective dissolution was shown to cause an increase in the thickness of the undissolved residue layer that is formed on the surface of slag particle. Precipitate layers of the resultant products were also observed on particle surfaces. These precipitates and residue layers caused increased resistance to diffusion from slag into the bulk solution. This type of selective dissolution that leaves behind undissolved residue

layers suggests a shrinking core mechanism. The nature of the dissolution in terms of mineralogical changes, e.g., formation of a residue layer, incongruent dissolution, and different extents of dissolution of different elements can indicate what could be the pros and cons of using a given slag for CO₂ sequestration. In our study, slag-2 shows high concentrations of dissolved mineral ions and less residue layers were observed which suggests a higher CO₂ sequestration potential than slag-1.

Initially, the concentration of dissolved ions grew, and eventually, it stabilized which revealed that there was a high dissolution rate during the first few hours of reaction; furthermore, significant quantities of Ca and Mg were extracted from the slag, compared to other minerals which indicate their high carbonation potential. Though Fe and Al can produce stable carbonates and were present within the slag in substantial quantities, their concentrations within solution were insignificant, which suggest that they do not contribute much to the carbonation process. The limited solubility of Fe and Al combined with the high pressure requirements of Mg carbonation supports the conclusion that Ca is the only element with substantial potential for carbonation under ambient conditions. The study also enables the identification of preferable slags for CO₂ sequestration through pure dissolution experiments. For instance, in this study, slag-2 is a better candidate for CO₂ sequestration simply because Ca contained in it dissolves faster than that in slag-1. The reduction of particle size in any sample yielded an increase in the rate of dissolution. It was observed that increasing the operating temperature from 25 to 90 °C yielded vast improvements in the rate of dissolution. Concentrations of toxic heavy metals in the leachate were found to be far below maximum acceptable limits as specified by CPCB.

These experiments provide a useful base case regarding the dissolution behavior of the slag into an aqueous medium. The dissolution rate without the presence of CO₂ will serve as a quantitative reference with respect to any study in which CO₂ is present, so that it can be estimated how much faster slag dissolves in the presence of CO₂ relative to the case when it is absent.

Acknowledgements This study is partially funded by a grant from Consortium for Clean Coal Utilization, McDonnell Academy, St. Louis, USA.

References

- Bacocchi R, Costa G, Poletini A et al (2009) Comparison of different reaction routes for carbonation of APC residues. *Energy Procedia* 1: 4851–4858. doi:10.1016/j.egypro.2009.02.313
- Bao W, Li H, Yi Z (2010) Selective leaching of steelmaking slag for indirect CO₂ mineral sequestration. *Ind Eng Chem Res* 49:2055–2063. doi:10.1021/ie801850s

- Bertos MF, Li X, Simons SJR et al (2004) Investigation of accelerated carbonation for the stabilisation of MSW incinerator ashes and the sequestration of CO₂. *Green Chem* 6:428–436. doi:10.1039/b401872a
- Bobicki ER, Liu Q, Xu Z, Zeng H (2012) Carbon capture and storage using alkaline industrial wastes. *Prog Energy Combust Sci* 38:302–320. doi:10.1016/j.pecs.2011.11.002
- Bonenfant D, Kharoune L, Sauve S et al (2008) CO₂ sequestration potential of steel slags at ambient pressure and temperature. *Ind Eng Chem Res* 47:7610–7616. doi:10.1021/ie701721j
- Bonfils B, Julcour-Lebigue C, Guyot F et al (2012) Comprehensive analysis of direct aqueous mineral carbonation using dissolution enhancing organic additives. *Int J Greenh Gas Control* 9:334–346. doi:10.1016/j.ijggc.2012.05.009
- Butt DP, Lackner KS, Wendt CH et al (1996) Kinetics of thermal dehydroxylation and carbonation of magnesium hydroxide. *J Am Ceram Soc* 79:1892–1898. doi:10.1111/j.1151-2916.1996.tb08010.x
- Chang EE, Chiu AC, Pan SY et al (2013) Carbonation of basic oxygen furnace slag with metalworking wastewater in a slurry reactor. *Int J Greenh Gas Control* 12:382–389. doi:10.1016/j.ijggc.2012.11.026
- Costa G, Polettini A, Pomi R, Stramazzo A (2016) Leaching modelling of slurry-phase carbonated steel slag. *J Hazard Mater* 302:415–425. doi:10.1016/j.jhazmat.2015.10.005
- CPCB (2006) Assessment of utilisation of industrial solid wastes in cement manufacturing. Central Pollution Control Board, Ministry of Environment & Forests, Govt. of India
- Daval D, Martinez I, Corvisier J et al (2009) Carbonation of Ca-bearing silicates, the case of wollastonite: experimental investigations and kinetic modeling. *Chem Geol* 262:262–277. doi:10.1016/j.chemgeo.2009.01.022
- De Windt L, Chaurand P, Rose J (2011) Kinetics of steel slag leaching: batch tests and modeling. *Waste Manag* 31:225–235. doi:10.1016/j.wasman.2010.05.018
- Diener S, Andreas L, Herrmann I et al (2010) Accelerated carbonation of steel slags in a landfill cover construction. *Waste Manag* 30:132–139. doi:10.1016/j.wasman.2009.08.007
- Eloneva S, Said A, Fogelholm CJ, Zevenhoven R (2012) Preliminary assessment of a method utilizing carbon dioxide and steelmaking slags to produce precipitated calcium carbonate. *Appl Energy* 90:329–334. doi:10.1016/j.apenergy.2011.05.045
- Ghacham AB, Pasquier LC, Cecchi E et al (2016) CO₂ sequestration by mineral carbonation of steel slags under ambient temperature: parameters influence and optimization. *Environ Sci Pollut Res*. doi:10.1007/s11356-016-6926-4
- Gunning PJ, Hills CD, Carey PJ (2010) Accelerated carbonation treatment of industrial wastes. *Waste Manag* 30:1081–1090. doi:10.1016/j.wasman.2010.01.005
- Hong KJ, Tokunaga S (2000) Extraction of heavy metals from MSW incinerator fly ashes by chelating agents. *J Hazard Mater* 41:57–73. doi:10.1016/S0304-3894(00)00171-0
- Huijgen WJJ, Comans RNJ (2005) Mineral CO₂ sequestration by carbonation of industrial residues. Energy Research Centre of the Netherlands (ECN). Petten, The Netherlands
- Huijgen WJJ, Comans RNJ (2003) Carbon dioxide sequestration by mineral carbonation, literature review. Energy Research Centre of the Netherlands (ECN). Petten, The Netherlands
- Huijgen WJJ, Witkamp GJ, Comans RNJ (2006) Mechanisms of aqueous wollastonite carbonation as a possible CO₂ sequestration process. *Chem Eng Sci* 61:4242–4251. doi:10.1016/j.ces.2006.01.048
- Huijgen WJJ, Witkamp G-J, Comans RNJ (2005) Mineral CO₂ sequestration by steel slag carbonation. *Environ Sci Technol* 39:9676–9682. doi:10.1021/es050795f
- Huntzinger DN, Eatmon TD (2009) A life-cycle assessment of Portland cement manufacturing: comparing the traditional process with alternative technologies. *J Clean Prod* 17:668–675. doi:10.1016/j.jclepro.2008.04.007
- IPCC (2005) IPCC special report on carbon dioxide capture and storage. Cambridge University Press, Cambridge
- Johnson CA, Brandenberger S, Baccini P (1995) Acid neutralizing capacity of municipal waste incinerator bottom ash. *Environ Sci Technol* 29:142–147. doi:10.1021/es00001a018
- Kasuura H, Inoue T, Hiraoka M, Sakai S (1996) Full-scale plant study on fly ash treatment by the acid extraction process. *Waste Manag* 16:491–499. doi:10.1016/S0956-053X(96)00091-8
- Koljonen T, Siikavirta H, Zevenhoven R, Savolainen I (2004) CO₂ capture, storage and reuse potential in Finland. *Energy* 29:1521–1527. doi:10.1016/j.energy.2004.03.056
- Lackner KS, Butt DP, Wendt CH (1997) Progress on binding CO₂ in mineral substrates. *Energy Convers Manag* 38:S259–S264. doi:10.1016/S0196-8904(96)00279-8
- Lekakh SN, Rawlins CH, Robertson DGC et al (2008) Kinetics of aqueous leaching and carbonization of steelmaking slag. *Metall Mater Trans B Process Metall Mater Process Sci* 39:125–134. doi:10.1007/s11663-007-9112-8
- Li Z, Zhao S, Zhao X, He T (2012) Leaching characteristics of steel slag components and their application in cementitious property prediction. *J Hazard Mater* 199–200:448–452. doi:10.1016/j.jhazmat.2011.07.069
- Morone M, Costa G, Georgakopoulos E et al (2016) Granulation–carbonation treatment of alkali activated steel slag for secondary aggregates production. *Waste and Biomass Valorization*. doi:10.1007/s12649-016-9781-0
- O'Connor W, Dahlin D, Rush G et al (2005) Aqueous mineral carbonation, mineral availability, pretreatment, reaction parametrics, and process studies. National Energy Technology Laboratory, Office of Fossil Energy, US
- O'Connor WK, Dahlin DC, Nilsen DN et al (2000) Carbon dioxide sequestration by direct mineral carbonation with carbonic acid. *Proc 25th Int Tech Conf Coal Util Fuel Syst* 0–15
- Olajire AA (2013) A review of mineral carbonation technology in sequestration of CO₂. *J Pet Sci Eng* 109:364–392. doi:10.1016/j.petrol.2013.03.013
- Pan SY, Chang EE, Chiang PC (2012) CO₂ capture by accelerated carbonation of alkaline wastes: a review on its principles and applications. *Aerosol Air Qual Res* 12:770–791. doi:10.4209/aaqr.2012.06.0149
- Pan SY, Chiang PC, Chen YH et al (2013) Systematic approach to determination of maximum achievable capture capacity via leaching and carbonation processes for alkaline steelmaking wastes in a rotating packed bed. *Environ Sci Technol* 47:13677–13685. doi:10.1021/es403323x
- Park AHA, Fan LS (2004) CO₂ mineral sequestration: physically activated dissolution of serpentine and pH swing process. *Chem Eng Sci* 59:5241–5247. doi:10.1016/j.ces.2004.09.008
- Proctor DM, Fehling KA, Shay EC et al (2000) Physical and chemical properties of blast furnace, basic oxygen furnace and electric arc furnace steel industry slag. *Environ Sci Technol* 34:1576–1582
- Quina MJ, Bordado JC, Quinta-Ferreira RM (2008) Treatment and use of air pollution control residues from MSW incineration: an overview. *Waste Manag* 28:2097–2121. doi:10.1016/j.wasman.2007.08.030
- Revathy TDR, Palanivelu K, Ramachandran A (2015) Direct mineral carbonation of steelmaking slag for CO₂ sequestration at room temperature. *Environ Sci Pollut Res* 23:7349–7359. doi:10.1007/s11356-015-5893-5
- Sahu RC, Patel RK, Ray BC (2010) Neutralization of red mud using CO₂ sequestration cycle. *J Hazard Mater* 179:28–34. doi:10.1016/j.jhazmat.2010.02.052
- Sanna A, Uibu M, Caramanna G et al (2014) A review of mineral carbonation technologies to sequester CO₂. *Chem Soc Rev* 43:8049–8080. doi:10.1039/c4cs00035h
- Santos RM, Ling D, Sarvaramini A et al (2012) Stabilization of basic oxygen furnace slag by hot-stage carbonation treatment. *Chem Eng J* 203:239–250. doi:10.1016/j.cej.2012.06.155

- Sipilä J, Teir S, Zevenhoven R (2008) Carbon dioxide sequestration by mineral carbonation literature review update 2005–2007. Faculty of Technology, Heat Engineering Laboratory, Abo Akademi University, Finland
- Sorlini S, Sanzeni A, Rondi L (2012) Reuse of steel slag in bituminous paving mixtures. *J Hazard Mater* 209–210:84–91. doi:10.1016/j.jhazmat.2011.12.066
- Squires K, Wolf GH (2006) Carbon sequestration via aqueous olivine mineral carbonation: role of passivating layer formation. *Environ Sci Technol* 40:4802–4808. doi:10.1021/es0523340
- Teir S (2008) Fixation of carbon dioxide by producing carbonates from minerals and steelmaking slags. Doctoral Dissertation, Department of Energy Technology, Helsinki University of Technology, Finland
- Teir S, Eloneva S, Fogelholm CJ, Zevenhoven R (2007) Dissolution of steelmaking slags in acetic acid for precipitated calcium carbonate production. *Energy* 32:528–539. doi:10.1016/j.energy.2006.06.023
- van Oss HG (2015) Iron and steel slag. U.S. Geological Survey, Mineral Commodity Summaries, US
- van Zomeren A, van der Laan SR, Kobesen HBA et al (2011) Changes in mineralogical and leaching properties of converter steel slag resulting from accelerated carbonation at low CO₂ pressure. *Waste Manag* 31:2236–2244. doi:10.1016/j.wasman.2011.05.022
- Xiao LS, Wang R, Chiang PC et al (2014) Comparative life cycle assessment (LCA) of accelerated carbonation processes using steelmaking slag for CO₂ fixation. *Aerosol Air Qual Res* 14:892–904. doi:10.4209/aaqr.2013.04.0121
- Yan J, Moreno L, Neretnieks I (1997) The long-term acid neutralizing capacity of steel slag. *Stud Environ Sci* 71:631–640. doi:10.1016/S0166-1116(97)80246-4
- Yuen YT, Sharratt PN, Jie B (2016) Carbon dioxide mineralization process design and evaluation: concepts, case studies, and considerations. *Environ Sci Pollut Res* 1–22. doi: 10.1007/s11356-016-6512-9